Modelling and Analysis of Real-World Wind Turbine Power Curves: Assessing Deviations from Nominal Curve by Neural Networks

Article *in* Renewable Energy · March 2019

DOI: 10.1016/j.renene.2019.03.075

4 authors:

Ciulla Giuseppina
Università degli Studi di Palermo

Antonino D'Amico
Università degli Studi di Palermo

V. Di Dio
Università degli Studi di Palermo

Valerio Lo Brano
Università degli Studi di Palermo

Modelling and Analysis of Real-World Wind Turbine Power Curves: Assessing Deviations from Nominal Curve by Neural Networks

G. Ciulla*, A. D'Amico, V. Di Dio, V. Lo Brano
Università degli Studi di Palermo, Dipartimento di Ingegneria, Viale delle Scienze edificio 9, 90128 Palermo, Italia
*corresponding author: giuseppina.ciulla@unipa.it
e-mail: antonio.damico@deim.unipa.it, vincenzo.didio@unipa.it, lobrano@dream.unipa.it

ABSTRACT

The power curve of a wind turbine describes the generated power versus instantaneous wind speed. Assessing wind turbine performance under laboratory ideal conditions will always tend to be optimistic and rarely reflects how the turbine actually behaves in a real situation. Occasionally, some aerogenerators produce significantly different from nominal power curve, causing economic losses to the promoters of the investment. Our research aims to model actual wind turbine power curve and its variation from nominal power curve. The study was carried out in three different phases starting from wind speed and related power production data of a Senvion MM92 aero-generator with a rated power of 2.05 MW. The first phase was focused on statistical analyses, using the most common and reliable probability density functions. The second phase was focused on the analysis and modelling of real power curves obtained on site during one year of operation by fitting processes on real production data. The third was focused on the development of a model based on the use of an Artificial Neural Networks that can predict the amount of delivered power. The actual power curve modelled with a multi-layered neural network was compared with nominal characteristics and the performances assessed by the turbine SCADA. For the studied device, deviations are below 1% for the producibility and below 0.5% for the actual power curves obtained with both methods. The model can be used for any wind turbine to verify real performances and to check fault conditions helping operators in understanding normal and abnormal behaviour.

Keywords

Wind energy¸ power curve, producibility estimates, aero-generator, anemometric campaign, Artificial Neural Network

Nomenclature

a_n	Fourier coefficient
b_n	Fourier coefficient
E_g	annual delivered energy [kWh]
f_n	nominal frequency [Hz]
h_{eq}	equivalent hours [h]
I_n	nominal current [A]
P	wind turbine power [kW]
P_n	wind turbine nominal power [kW]
R.H.	relative humidity [%]
T	air temperature [°C]
U_n	nominal voltage [V]
v	wind speed [m/s]
V_{med}	average wind speed [m/s]
V_{Max}	maximum wind speed [m/s]
ρ	air density [kg/m^3]
ANN parameters	
A_i	activation potential
w_{ij}	interconnection synaptic weights between *i*-th and *j*-th neuron layers
x_i	neuron input data
y_i	neuron output data
α	momentum
Δ	estimated and actual power curve deviation
η	learning rate
Φ	neuron activation function

1. Introduction

Wind power is a key actor in the field of renewable energy sources. Production capacity has risen exponentially in recent years [1]. The wind energy in Europe, issuing about 10.4% of the electricity demand in 2016, is an important technology that can help in meeting the goals the EU has set itself to achieve a low carbon energy policy by 2050 [2]. Due to the shortage of traditional energy resources and ecological degradation of the environment, the generation of electricity from wind power has experienced rapid development [3,4]. Achieving the aforementioned goal in 2050 is made possible developing modern wind turbines with high levels of reliability and power production. Nonetheless, a reliable prediction of power production within a small margin of error has always been a major issue.

The amount of energy that a turbine can produce depends on several parameters including the wind regime of the specific site and the main characteristics of the wind turbine [4]: on the wind intensity and wind direction, on the rotor diameter and rotor height, on weather conditions such as temperature, density and air pressure, and also depends on the wind turbulence in the immediately preceding time. For this reason, the assessment of the site productivity is a preliminary crucial step in the wind farm realization.

Another fundamental step is to combine the anemometric studies with the power curves of the wind turbine supplied by the manufacturers, even to match between the wind turbine and the specific site in order to obtain maximum energy and reliability benefits [4]. An accurate assessment of the power generated by a wind turbine is important since expenses in operation and maintenance represent 10% of the total cost of any wind energy project [5].

The main parameter that represents the relationship between wind speed and the power output of a wind turbine [6] is the power curve, governed by a cubic relationship of these variables [7]. A comparison between measured power output versus power output given by the manufacturer power curve (MPC) shows a similar trend but with real data is always scattered. This is because, besides the wind speed, there are more important variables involved in turbine power output such as atmospheric pressure, turbulence intensity, wind direction variability, both vertical and horizontal shear, atmospheric stability, drive train temperature and so on [8]. Moreover, the standard conditions under which the MPC is derived are different from those under which the turbine is operated. Furthermore, local orography and wake effects produced by other turbines need to be taken into consideration in power estimations of wind farms in field conditions [7].

Several techniques have being used to model the turbine power curve: parametric [9], non-parametric [10,11] and stochastic [12] methods. In this context, several attempts have been made to identify a reliable model to assess the wind turbine power curve [13]. In [14,15] a discrete approximation approach is applied where the power delivered by the wind turbine, model output, is only a function of the hub wind speed and air density. However, in [8,16] it is recognized that other input parameters significantly influence the correct evaluation of the power output of a wind turbine. In [17] a parametric approach using a set of mathematical equations was tested.

Normally, wind power curves of each new turbine are obtained in wind tunnels on scale models; later, prototypes are tested directly on the field by the same manufacturing companies. Each company guarantee the power generation curves of the generator and the availability of its operation at exact percentages, often close to 100%. It is clear that a single percentage point of lower productivity can conduct to a loss of profit. If the production of the wind turbine differs negatively from the expected productivity, the investors can claim compensation due to economic losses. The mismatch among declared and actual wind power curve often results in contentious between investors and manufactures.

Another option to assess the WTPC is represented by Wind Turbine Condition Monitoring (WTCM) systems that are increasingly installed with the primary goal of providing wind turbine component specific information to wind farm operators to be used for optimal maintenance planning [18]. Their economic benefit to operation and maintenance costs has been investigated [19,20], and proven to be substantial although it largely depends on the fault detection rate [21]. While many commercial solutions, techniques and methods are available [22,23], their related cost and complexity deter operators from a widespread deployment [24]. The use of data from the Supervisory Control And Data Acquisition (SCADA) system appears therefore as a potential solution for WTCM due to its availability at no additional cost. The SCADA system usually samples data at relatively high frequency (typically 1 Hz) with standard practice to store 10-min averaged values of the parameters characterising the operating and environmental conditions.

There are a small number of works in the literature in which authors use the non-parametric methods for example through the application of artificial intelligence-based tools to model the wind turbine power curve as a power performance validation tool. Artificial Neural Networks (*ANN*) have been demonstrated to be well suited for solving nonlinear problems with multiple input variables [25] and, as such, have been successfully applied to the prediction of wind speed and power generated by wind farms.

In [26], the authors used experimental data collected from three wind farms in Southern Italy and trained a two-hidden layer neural network to predict the wind energy output; in [27], field data collected from seven wind farms were used for the analysis and prediction of power generation from wind farms, developing a neural network with three input (wind speed, relative humidity and generation hours) and one output, the energy output of wind farms. In the study [28], it is demonstrated that the neural network based Measure-Correlate-Predict (MCP) method performs very well respect to the correlation, root-mean-square error and the distance in the wind speed frequency distribution . In [13] the authors use the *ANN* for modelling the power curve of a wind turbine located in a specific site, in [29] use the genetic algorithm, in

[27,30] developed an *ANN* model to determine the delivered power of wind power plant, in [31] was proposed a dynamic model based on RBF neural network to consider the nonlinear time-variant essence of wind power generation systems.

The purpose of this study is to explore the possibility of generating a WTPC using artificial intelligence techniques such as neural networks and using data from real installations. The tool should provide to wind farm managers the opportunity to compare the real WTPC with the data provided by the manufacturer and thus be helpful in any disputes arising from productivity indices lower than expected. The authors then investigated power output time series of a real wind turbine SEVION MM92, being part of a wind farm installed in Southern Italy, comparing the performances declared in the technical datasheet.

After a preliminary statistical analyses of input data, the authors extracted the actual power curve of the wind turbine for different air density ranges and with a bin of 0.10 m/s. In order to compare this curve with the curve provided by manufacturer, two different methods have been applied to fit the manufacturer curve at the same bin: spline interpolation and Fourier series interpolation function. In the last part of the paper the authors, employing an *ANN* and an optimization technique based on the application of a Genetic Algorithm (GA), created a model that returns a WTPC from real data. The reliability of this model was confirmed by the low value of the Standard deviation of about 44 kW respect to the nominal power of 2050 kW of the examined turbine. Furthermore, the developed neural network model takes into account a significantly higher number of variables related to the description of the phenomenon (ten input data and one output data) respect conventional and/or statistical models.

2. Anemometric campaign

The use of wind as a source of kinetic energy for the electricity production is subordinated to the occurrence of a several conditions that make the installation of wind farm competitive and profitable. For this reason, a preliminary feasibility study is always accompanied by an anemometric campaign. Our study employs an annual anemometric campaign linked to a wind turbine.

Two anemometers have been used: one anemometer is located in the wind farm and another is located over wind turbine. For security and privacy reasons details about position and property of the wind plant cannot be disclosed. However, we can say that the wind farm is located in southern Italy and that the area is characterized by a simple and flat orography, free of natural obstructions. The SENVION MM92 generator (WTG test) used in this study is located about 500 m from the anemometric station and about 800 meters from the other nearby turbines (Fig. 1).

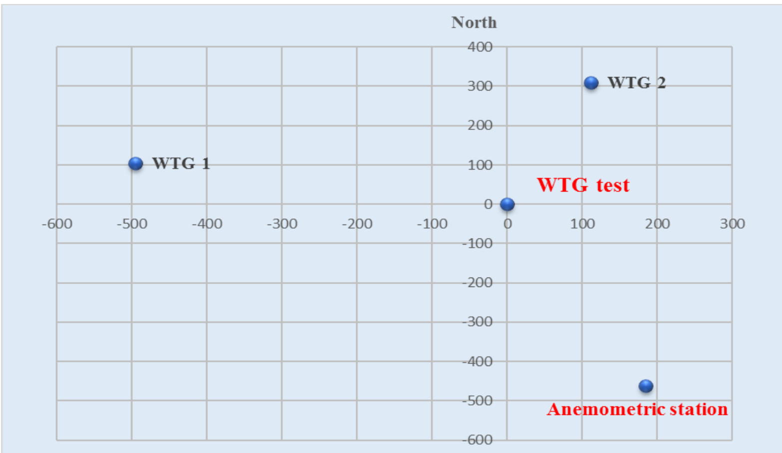

Fig. 1. Aero-generators and anemometric station positions.

The main variables measured by the anemometric station at different heights are: maximum, average and minimum wind speeds, standard deviation, wind direction, air temperature, relative humidity and atmospheric pressure with a time step of 10 minutes. In Fig. 2 are shown the daily wind speed trends, measured by the anemometer and by the WGT anemometer of the turbine.

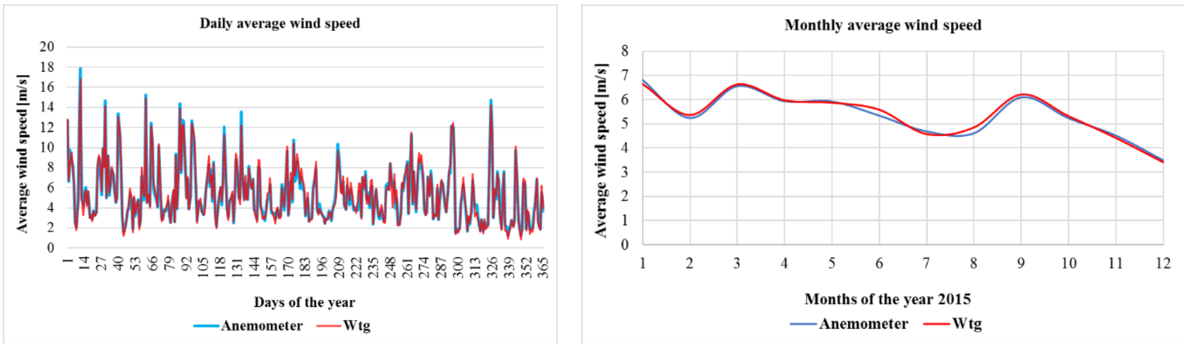

Fig. 2. Wind speed trends at different time steps.

Fig. 3 shows the average, maximum and minimum wind speed and the standard deviation (StD) at 82 meters a.s.l. (the highest point); this site is characterized by an annual average wind speed of 5.37 m/s.

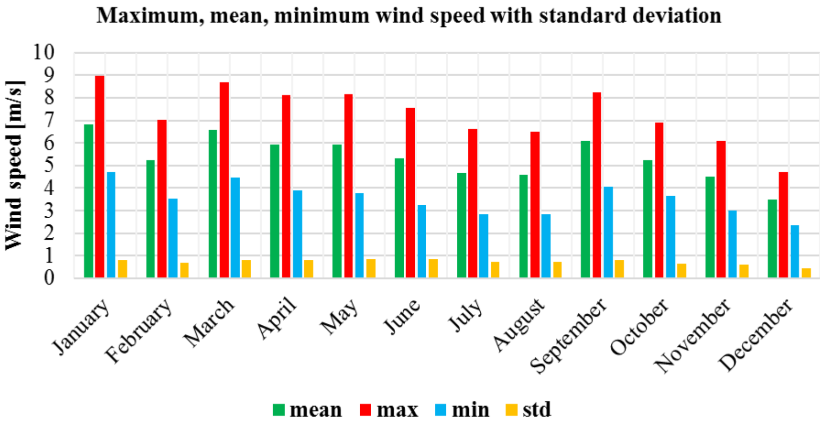

Fig. 3. Average, maximum and minimum wind speed and StD.

The maximum and minimum wind speed values are almost equidistant from the average value: this means that the site is not characterized by a high level of wind turbulence.
Fig. 4 shows the 2D wind rose and a 3D representation that also considers the intensity of wind with direction.

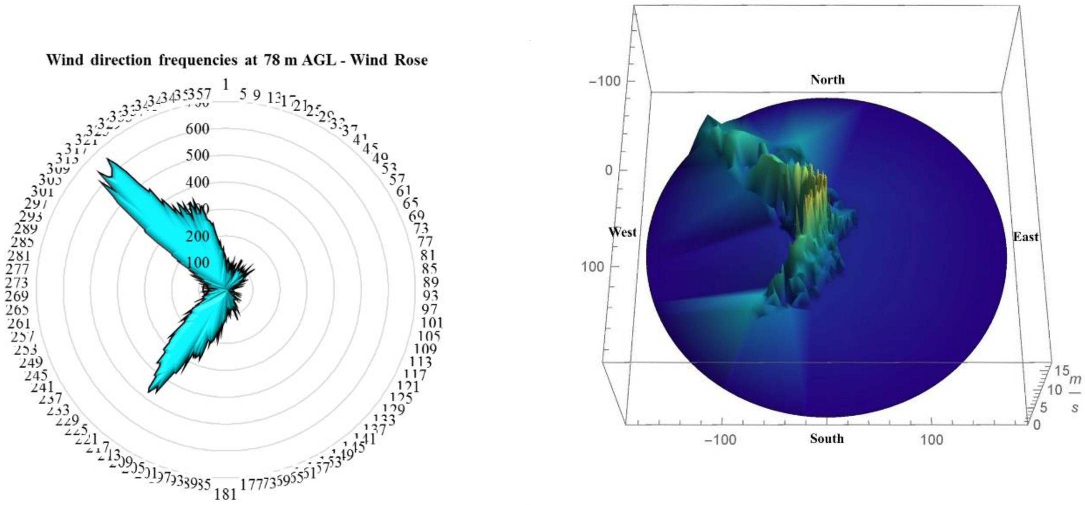

Fig. 4. 2D and 3D wind roses.

Data clearly shows that Mistral (north-westerly wind) represents the most frequent direction; on the other hand, Libeccio (westerly or south-westerly wind) issues wind with the greatest intensity; all other wind directions are rarely detected (Fig. 5).

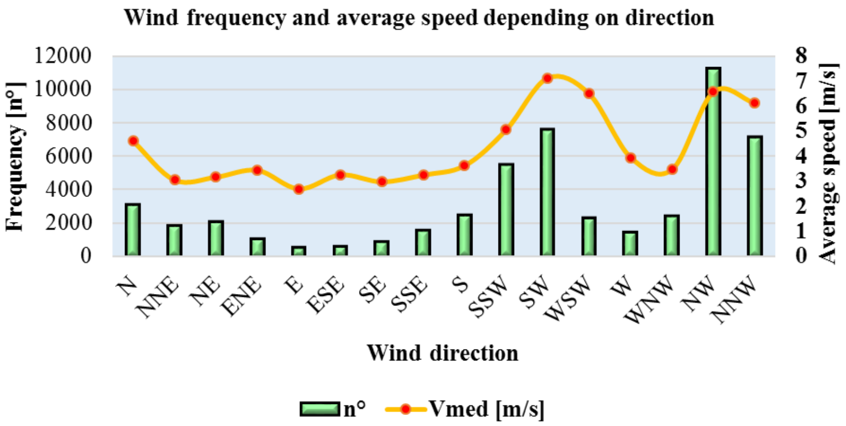

Fig. 5. Frequency distribution and average wind speed.

In addition to wind speed and direction data, even air density (ρ) was considered; to improve the accuracy of models we used a variable air density calculation with a time step of 10 minute (Fig. 6).

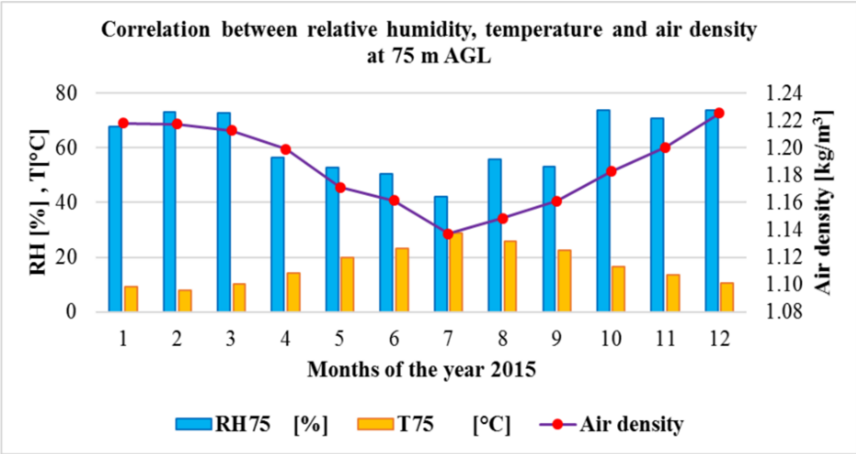

Fig. 6. Monthly average temperature, density and humidity of the air at 75 meters above ground level.

2.1. Statistical analysis of wind data

A pre-processing phase was performed on the 10-min average data series to eliminate invalid data points [32]. In the following, the most important parameter is the average wind speed measured at the maximum height, the nearest to the real turbine rotor height. Then, because the reliability and goodness of a site producibility analysis depends on the fitting of the Probability Density Functions (PDF), a statistical analysis was carried out by using fitting algorithms to adapt data-points to PDF. Due to the nature of the data processed, Weibull and Burr PDF were chosen.

The Weibull distribution is one of the most widely used statistical distributions in reliability engineering and wind speed analysis; on the other hand the Burr distribution has been recently applied to wind speed problems with good results. In [33], three types of probability distributions have been used to estimate the wind energy potential in Malaysia; a comparison shows that of all the three distributions used, Burr distribution provides the best fit. In [34], the study investigates the wind speed characteristics recorded in the urban area of Palermo, in the south of Italy, by a monitoring network composed by four weather stations. Even in this case the results show that, concerning the accuracy of fitting the empirical data, Burr PDF has the best agreement.

Figs. 7 and 8 show the Weibull and Burr distribution fitting over the experimental data concerning average wind speed and linked cumulative function.

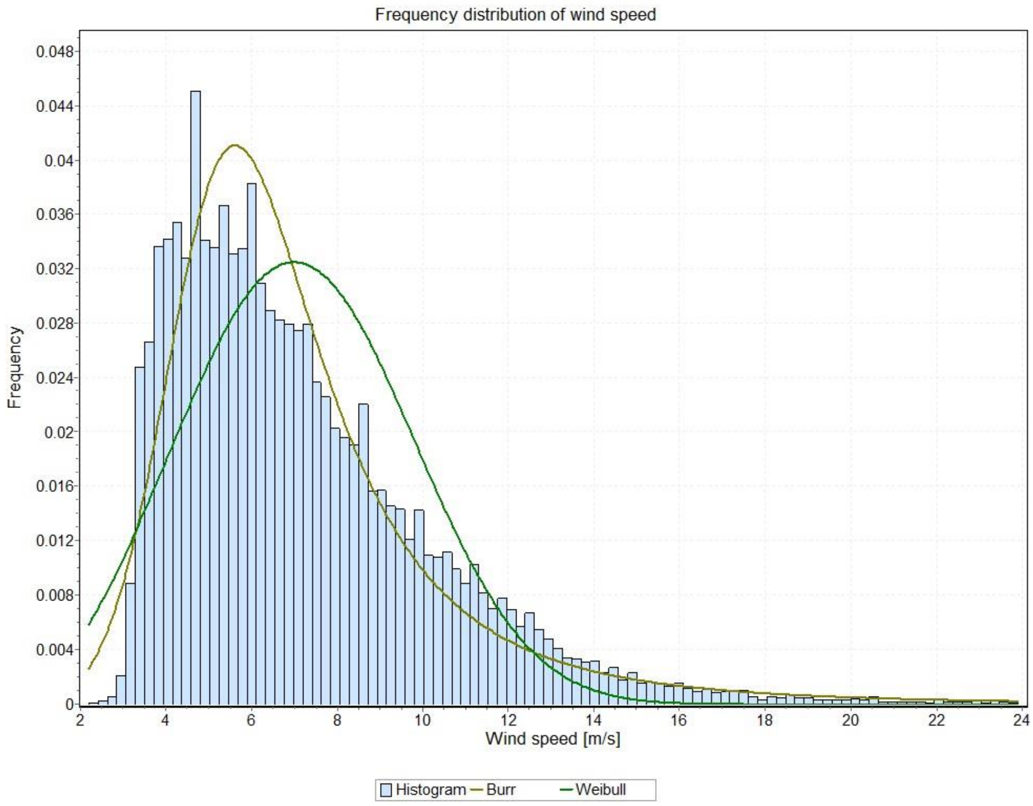

Fig. 7. Weibull and Burr distribution fitting over experimental frequency distribution of average wind speed.

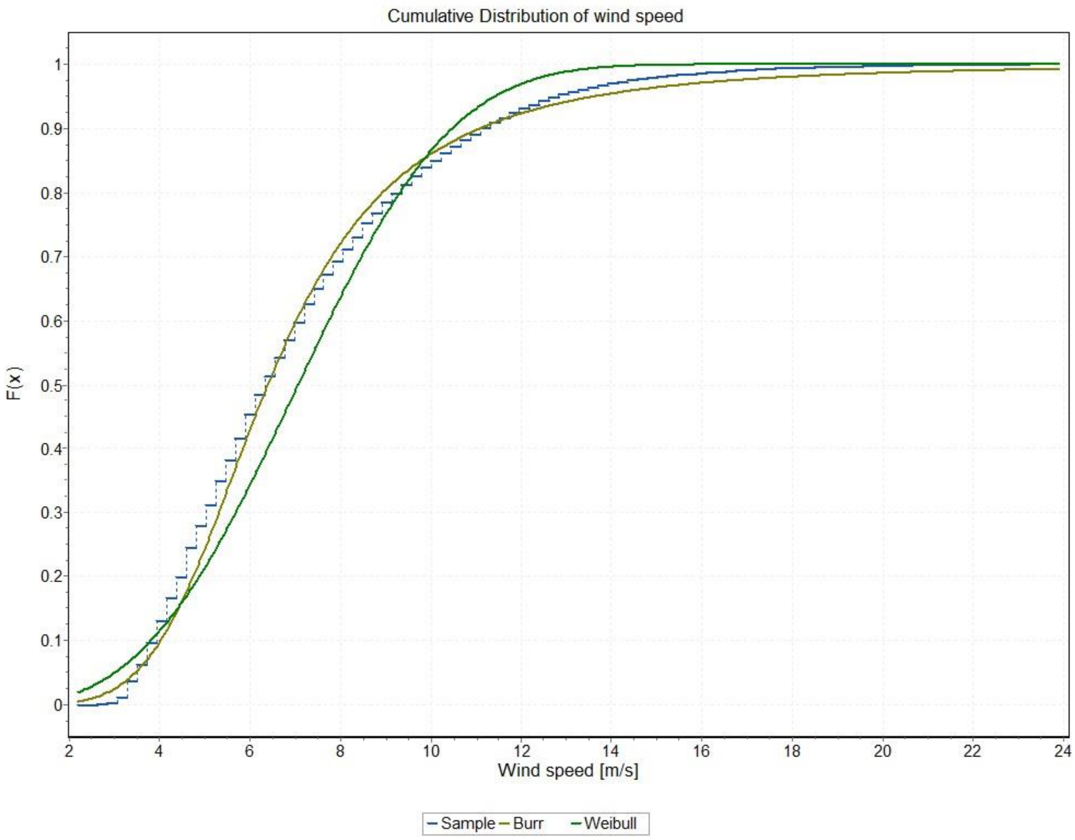

Fig. 8. Weibull and Burr cumulative fitting over experimental data of average wind speed.

Table 1 show the equations and the parameters value of Weibull and Burr distribution for the probability density function and survival function of average wind speed respectively in which α is the shape or slope parameters, β and k are the scale parameters.

Table 1: Equations and parameters value of Weibull and Burr distribution.

PDF parameters		
	Weibull distribution	**Burr distribution**
PDF	$f(x)=(\alpha/\beta^{\alpha})\cdot x^{\alpha-1}\cdot e^{-(x/\beta)^{\alpha}}$	$f(x)=\frac{\alpha\cdot k}{\beta}\cdot\left(\frac{x}{\beta}\right)^{\alpha-1}\cdot\left[1+\left(\frac{x}{\beta}\right)^{\alpha}\right]^{-k-1}$
Cumulative Function	$F(x)=1-e^{-(x/\beta)^{\alpha}}$	$F(x)=1-\left[1+(x/\beta)^{\alpha}\right]^{-k}$
Survival Function	$S(x)=e^{-\left(\frac{x}{\beta}\right)^{\alpha}}$	$S(x)=\left[1+\left(\frac{x}{\beta}\right)^{\alpha}\right]^{-k}$
k	-	4.2461
α	1.5644	1.8049
β	5.9977	12.061

3. Case study

Wind turbines assures their maximum performances under nominal and constant operating conditions and obviously, these conditions can be achieved only in a wind tunnel. Indeed, as seen before, the wind and its related variables are almost never constant. Other operating parameters that can be used to study the actual behaviour of the wind turbines are:

- wind speed turbulence percentage, defined as the ratio of the standard deviation of the wind speed and its average value in the ten-minute interval;
- wind direction turbulence percentage, defined as the ratio of the standard deviation of the wind direction and its average value in the ten-minute interval;
- wind speed gust ratio, defined as the ratio between the maximum value of the wind speed in the ten-minute interval and the average value of the speed, in the same interval;
- wind specific power, defined as power flowing through the surface unit perpendicular to the velocity wind trajectory, $P_w = 0.5\cdot\rho\cdot v^3$;
- wind specific energy.

The used dataset is related to an anemometric campaign linked to a SENVION MM 92 turbine with a nominal power of 2050 kW, a rotor diameter of 92.5 m and an electric pitch regulation system on each blade. In Table 2 are shown the main technical features of the wind turbine.

Table 2: Main features of the SENVION MM92 turbine.

Data sheet SENVION MM92	
Nominal power	P_n = 2050 [kW]
Nominal voltage	U_n = 690 [V]

Nominal current	I_n = 1715 [A]
Nominal frequency	f_n = 50 [Hz]
Rotor diameter	92.5 [m]
Blades length	42.5 [m]
High tower	100 [m]
Total high	146.3 [m]

In the dataset issued by the wind farm owner the power output from the wind generator is averaged over steps of 10 minutes; over 52460 recorded data points the wind turbine has provided electrical power in 34445 points, equivalent to 5740 operating hours; the generator has been inactive or absorbing energy from the grid for 18015 intervals, equal to 3002 hours. These hours are not to be confused with the concept of equivalent hours (h_{eq}) which is nothing more than the dummy number of hours in which the wind turbine should work at its nominal power to deliver an amount of electricity equal to that delivered in the same year operating at different power levels depending on wind speed, defined as:

$$h_{eq} = \frac{E_g}{P_n} \qquad \textbf{(1)}$$

where E_g is the energy delivered in a year by the generator [kWh], P_n is nominal power of the wind turbine [kW].

3.1. Power curve issued by manufacturers

The power curves issued by the manufacturers provide the user the theoretical performances with wind speed changes. Fig. 9 shows the manufacturer WTPC of the SENVION MM92 turbine.

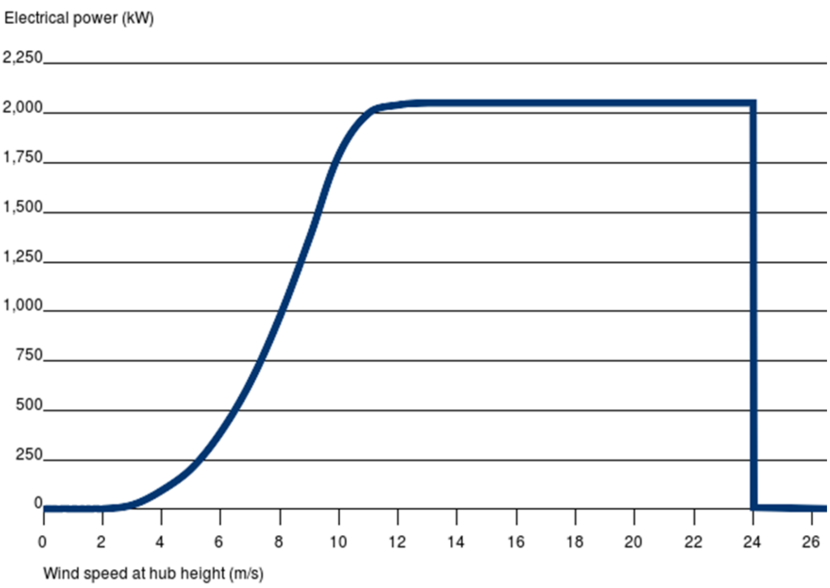

Fig. 9. Graphical WTPC issued by manufacturer related to the air density value of 1.225 kg/cm^3.

Obviously, the power output increases as the density increases as shown in Fig. 10;

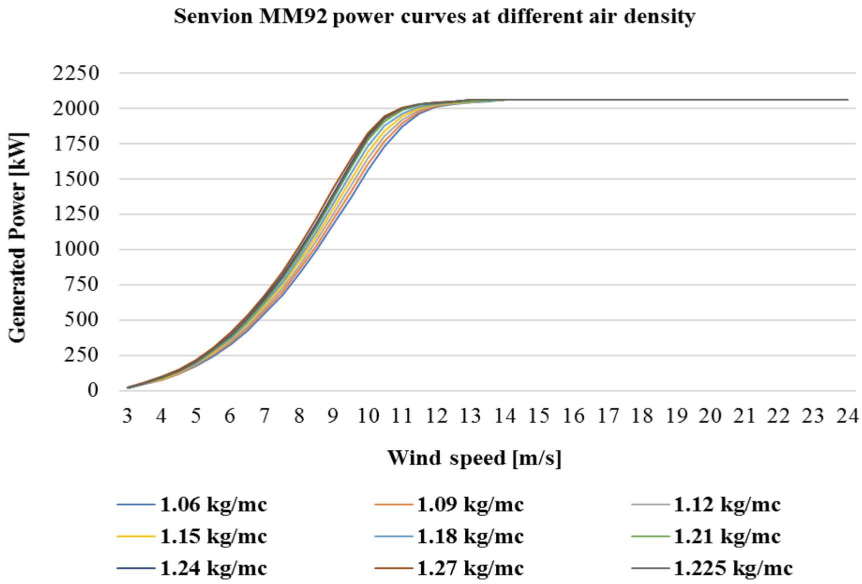

Fig. 10. WTPC variation with air density.

3.2. Producibility assessment

In order to facilitate the comparison between data coming from statistical or neural models with official data issued by manufacturers (data often provided in tabular form or in graphical form), it is advisable to adopt a methodology that allows to derive from the datasheets an analytical form of the WTPC. To this aim, to analyse the behaviour of the exanimated turbine and to carry out an accurate producibility assessments, the authors decided to reduce the wind speed bin of the official WTPC of a factor 10; from 1 to 0.1 m/s, obtaining more accurate curves. Two methods of numerical interpolation have been used:

- Spline interpolation function;
- Fourier series.

The two methods are employed to transform the official WTPC usually provided by the manufactures in histograms or tables form with a resolution of 1 m/s, in an analytical function, easier to use when comparing with other curves.

3.2.1 Spline interpolation function

The spline function is a special interpolation method that uses polynomial equations. Its application involves subdividing the interpolation interval into sub-intervals and interpolating the starting function in each of them trough low degree polynomials. This approach allows to solve the difficulties encountered when trying to interpolate the whole function with a single high degree polynomial. In the case study examined in the paper, the interpolation interval $[0, V_{\max}]$ of the power output function has been divided into sub-intervals through the following nodes succession:

$$\Delta_m = \{0 = v_0 < v_1 < ..... < v_n = V_{\max}\} \quad \textbf{(2)}$$

The authors, to perform the interpolation of the data set, used a natural cubic spline that is a third-degree polynomial in each interval $[v_i, v_{i+1}]$ with $i = 0,1,...,n-1$. The form of each cubic spline in $[v_i, v_{i+1}]$ is:

$$P(v) = a \cdot v^3 + b \cdot v^3 + c \cdot v + d \quad \textbf{(3)}$$

in which the coefficients *a*, *b*, *c*, *d* are calculated imposing the following constraints:

1. the $P(v)$ assumes the values $P(v_i)$ and $P(v_{i+1})$;
2. the tangent to the curve at the point $[v_i, P(v_i)]$ forms equal angles with the segments joining $P(v_i)$ to $P(v_{i-1})$ and $P(v_i)$ to $P(v_{i+1})$.

3.2.2 Fourier series interpolation

Fixed the value of the air density, the function $P(v)$ allows to calculate the delivered power by the wind turbine varying the wind speed value. This function is considered periodic, limited and integrable in the period [0, V_{max}]. The Fourier series development of this function, arrested at the eighth order is given by the following equation:

$$P(v) = a_0 + \sum_{n=1}^{8} \left[a_n \cdot \cos\left(\frac{2\pi \cdot n}{V_{max}} \cdot v \right) + b_n \cdot \sin\left(\frac{2\pi \cdot n}{V_{max}} \cdot v \right) \right] \quad \textbf{(4)}$$

where a_0, a_n and b_n are Fourier coefficients defined by the following equations:

$$a_0 = \frac{1}{V_{max}} \int_0^{V_{max}} P(v)\,dv \quad \textbf{(5)}$$

$$a_n = \frac{2}{V_{max}} \int_{-V_{max}}^{V_{max}} P(v) \cdot \cos\left(\frac{2\pi \cdot n}{V_{max}} \cdot v \right) dv \quad \textbf{(6)}$$

$$b_n = \frac{2}{V_{max}} \int_{-V_{max}}^{V_{max}} P(v) \cdot \sin\left(\frac{2\pi \cdot n}{V_{max}} \cdot v \right) dv \quad \textbf{(7)}$$

The two methods concisely introduced above, permits to generate a WTPC from tabular technical datasheet with a wind speed step of 0.1 m/s, and a comparative analysis of the results obtained with the two methods is performed. The process has been applied of each official dataset varying with air density. The results showed that the reliability of the “enriched” WTPC obtained by the two methods is high and the two curves are practically superimposed except for the initial part. As shown in Fig. 11, only for low wind speed there is a small difference. However, comparing the two curves obtained by the two methods with the graphical WTPC issued by the manufacturer, it can be seen that in this zone the power curve obtained with the spline interpolating function slightly overestimates the power output.

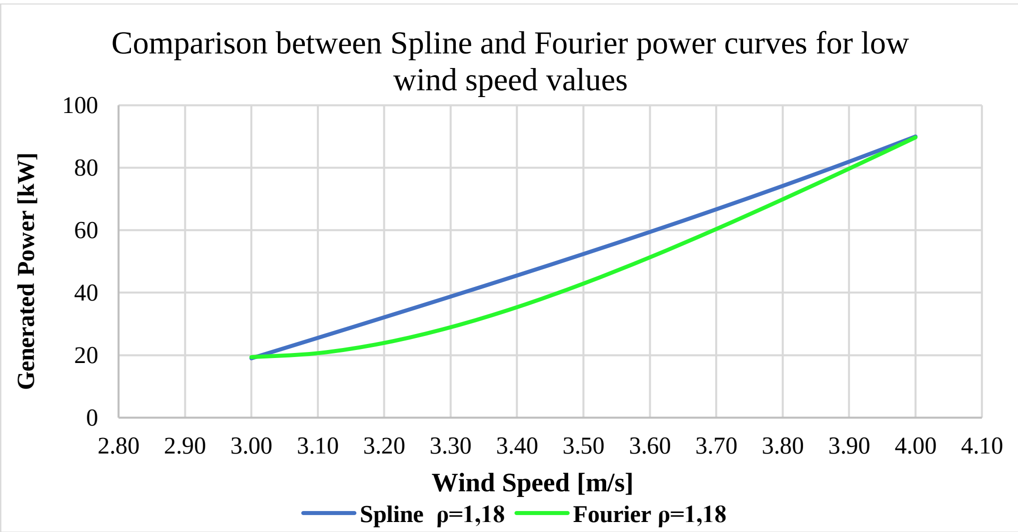

Fig. 11. Comparison between Spline and Fourier power curves with air density of 1.186 [kg/m^3].

Therefore, it has been assumed that the enriched WTPCs generated by the Fourier series method, although more complex and more expensive in terms of computational load, are more adequate than WTPC generated by cubic spline.

The producibility assessment, collected in Table 3, was made by using the enriched WTPC obtained by Fourier series interpolation applied to official data and for an mean air density of 1.186 [kg/m^3]. The generated energy (E_g) and the number of equivalent hours (h_{eq}) were calculated changing the wind detection height. In bold are underlined the data monitored at 103 m of altitude measured contemporary from hub anemometer and park anemometer.

Table 3: Producibility assessment by Fourier series applied to official WTPC.

Producibility assessment			
Anemometric station	**Height**	E_g	h_{eq}
	[m]	**[MWh]**	**[h]**
Hub anemometer	**103**	**4,357.22**	**2,125.48**
Park anemometer	**103**	**4,217.14**	**2,057.14**
Park anemometer	82	4,027.35	1,964.56
Park anemometer	80	3,901.14	1,903.00
Park anemometer	60	3,746.29	1,827.46
Park anemometer	40	3,629.01	1,770.25

To compare the above evaluation with the real productivity, the authors decided to use the wind data recorded with the hub anemometer (Table 4).

Table 4: Comparison between actual and estimated producibility.

Producibility				
	Anemometric station	**Height**	E_g	h_{eq}
		[m]	**[MWh]**	**[h]**
WTG Sevion MM92	**Hub anemometer**	103	3,988.87	1,945.79
Power curve issued by manufacture	**Hub anemometer**	**103**	**4,357.22**	**2,125.48**

In this case, the power curve issued by manufactured conducts to an overestimation of 8% of the actual production of energy. If we exclude a discrepancy between the actual and the officially declared characteristics of the turbine, the differences, in terms of generated energy and equivalent hours, could be attributed to the following machine stop reasons:

- maintenance, TERNA (an Italian electricity transmission system operator) dispatching and realignment;
- average wind speed next to the cut-off wind speed;
- average wind speed next to the cut-in wind speed.

3.3. Extraction of experimental WTPC

In the wind practice, given the manufacturers WTPC, and given the analyses produced in the anemometric campaigns, it is possible to evaluate the producibility of the aerogenerator. Anyway, the mismatch among declared and actual WTPC often results in contentious between investors and manufactures. Consequently, the aim of this work is to deploy a mathematical tool capable of demonstrating whether an installed aerogenerator produces in accordance with what is stated in the technical datasheets. The first step was to group the actual power output versus the contemporary wind speed value. As expected, the points are distributed on a sigmoid curve (Fig. 12).

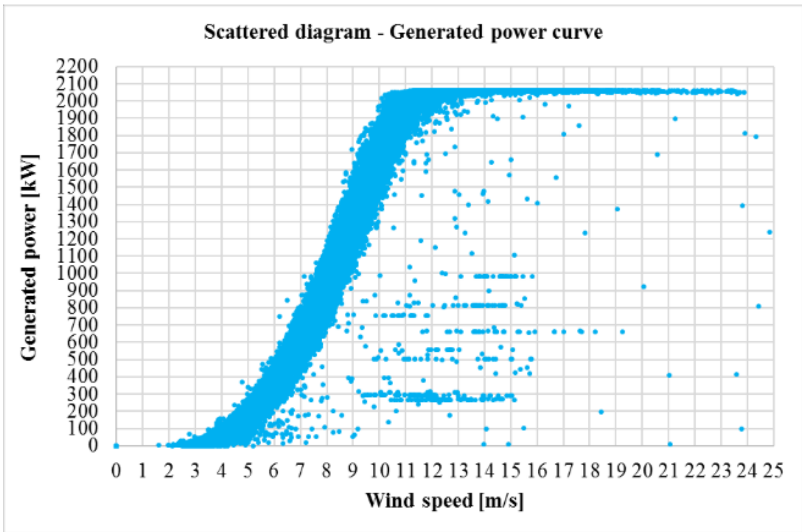

Fig. 12. Actual wind turbine power output vs wind speed.

In a simplified approach, since each operating condition is a function of only two variables, velocity and density of air, it is possible to obtain the mathematical function representing the WTPC for the given air density applying a mathematical model (such as those described in section 3.2) exploiting data and applying Ordinary Least Squares (OLS) technique. To deploy an experimental WTPC the authors followed two different approaches; the first based on a simplified mathematical model based on an interpolation procedure with OLS application, the second based on a complex model that exploits the learning ability of an artificial neural network.

4. Experimental WTPC with simplified approach

The first operation was to remove from the previous graph all those abnormal operating conditions that can be defined as outliers of the dataset. Then, the dataset was reduced from 52460 to 33429 values, as depicted in (Fig. 13).

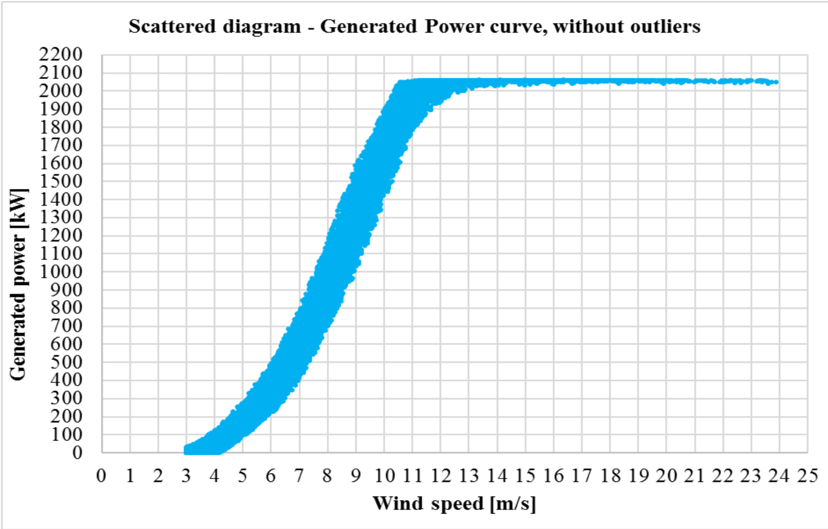

Fig. 13. Actual wind turbine power output vs wind speed without outliers.

Data points of the reduced dataset have been used in a curve fitting procedure, a process of constructing a curve, or mathematical function, that has the best fit to a series of data points.

4.1 Experimental WTPC with cubic spline interpolation

In our implementation, the OLS method has been applied to set of third order curves in Matlab environment. The computational load is significantly affected by the number of points to which the OLS method has to be applied. In our case the application of Fourier series interpolation requires a much higher calculation time and, considering the minimum deviation shown in Fig. 11, the cost / benefit ratio has led us to choose the cubic spline in comparison with Fourier series.

Three distinct simplified models have been defined:

1. Model 1 is a model that allows to determine WTPCs depending on both the speed and the air density. The air density range used in the model 1 is: (1.12-1.24 kg/m^3);
2. Model 2 is a model that allows to determine the WTPC depending on wind speed and for given average air density value recorded in the reference year (1.186 kg/m^3);
3. Model 3 is a model that allows to determine the WTPC depending on wind speed and two different air density values, summer average air density value and winter average air density value.

The comparison between the WTPCs obtained from the models and the WTCPs issued by the manufactures demonstrates a high corresponds. As example, in Fig. 14 is illustrated the comparison between the WTPC obtained by the Model 2 curve fitting procedure (red curve) versus the manufacturers WTPC obtained in section 3.2 considering constant the air density and equal to 1.186 kg/m^3 with wind speed step of 0.1 m/s (green line).

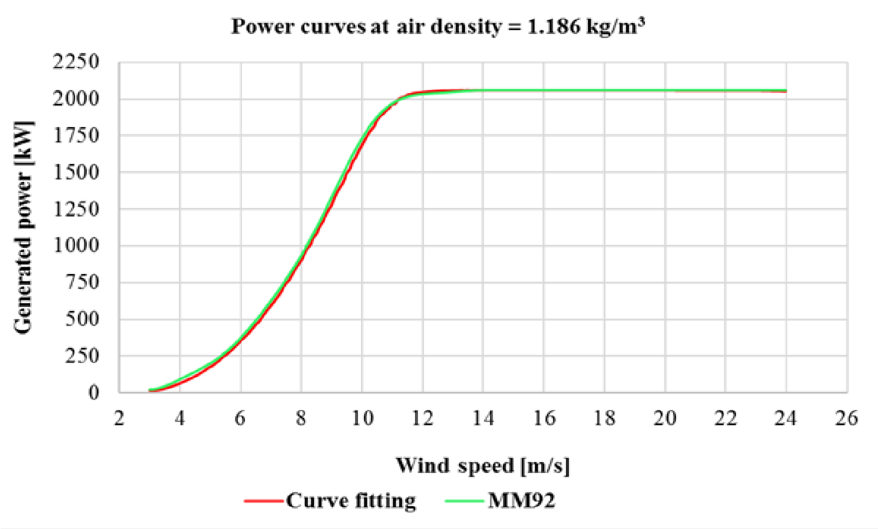

Fig. 14. Model 2 and manufacturer WTPC.

The graph shows a very good relationship between the results of the implemented mathematical model with manufacturer data. This means that the wind turbine model under examination has a very good compliance with official datasheet.

4.2 Experimental WTPC with Fourier series interpolation

Concerning the generation of WTPC using real data and applying Fourier series interpolation, this operation has been implemented on the SCADA control system of the aero-generator that allows to extract, on the basis of the data measured in a year, the experimental WTPC in a tabular form. In Table 5 are compared the results obtained with Model 2 and those obtained with Fourier series interpolation.

Table 5: Comparison between experimental Fourie WTPC and experimental cubic spline WTPC (Model 2) with wind speed step of 1 m/s.

Comparison between experimental WTPC for air density 1.186 kg/m³							
V_{med}	**FOURIER (8 harmonics)**	**CUBIC SPLINE**	**Δ**	V_{med}	**FOURIER (8 harmonics)**	**CUBIC SPLINE**	**Δ**
[m/s]	**[kW]**	**[kW]**	**[%]**	**[m/s]**	**[kW]**	**[kW]**	**[%]**
3.00	13.97	15.00	7.35	14.00	2057.29	2057.79	0.02
4.00	70.32	67.83	-3.54	15.00	2057.21	2057.42	0.01
5.00	177.03	178.20	0.66	16.00	2057.46	2057.59	0.01
6.00	344.67	349.15	1.30	17.00	2055.56	2057.92	0.11
7.00	586.90	585.67	-0.21	18.00	2058.00	2058.00	0.00
8.00	894.30	896.06	0.20	19.00	2057.55	2057.55	0.00
9.00	1267.59	1273.01	0.43	20.00	2057.29	2057.29	0.00
10.00	1634.88	1673.60	2.37	21.00	2056.20	2056.20	0.00
11.00	1929.67	1950.85	1.10	22.00	2055.32	2055.32	0.00
12.00	2034.96	2042.33	0.36	23.00	2056.21	2056.21	0.00
13.00	2052.98	2055.68	0.13	24.00	2051.67	2051.67	0.00
Δ Average value for different wind velocity range							

wind speed range	**3 - 24 [m/s]**	0.47%
wind speed range	**10 - 24 [m/s]**	0.27%
wind speed range	**13 - 24 [m/s]**	0.02%

Where Δ represent the percentage deviation between the Fourier and cubic spline WTPC.

5. Experimental WTPC with Artificial Neural Network

An ANN is a mathematical model consisting of artificial neurons that is inspired by a real biological neural network. Artificial neurons are arranged in layers and exchange information with other neurons and/or with themselves and interconnections define the topology of ANN [35]. The ANNs can be used to simulate complex relationships between inputs and outputs that other analytic functions cannot represent [36,37]. Indeed, an ANN receives external signals on a layer of input nodes, each of which is connected with numerous internal nodes, organized in multiple layers. Each node processes the received signals through its activation function *(Φ)* [38] and transmits the result to subsequent nodes as schematically shown in Fig. 15.

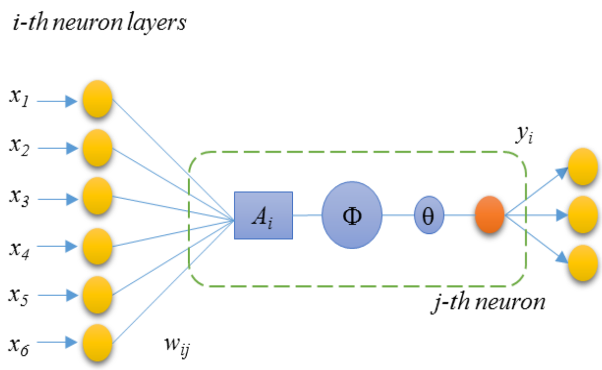

Fig. 15. Artificial neural network scheme [35].

In an ANN, the link between input and output is not defined by explicit relationships but is obtained through an empirical training process based on the presentation of matching input and outputs patterns. In most cases, it is an adaptive system that changes its structure in relation to external information flowing through the network during the learning phase [35]. The training algorithm modifies some network parameters at each iteration to get the desired response from the analysed phenomenon (supervised learning mode). These parameters are the numerical weights (w_{ij}) associated with the synaptic connections between the neurons of the network.
A dataset of actual input and output examples is used: in this case the dependent variable, the output power of the wind turbine, is a function of one or more independent variables. To the aim to internally validate the ANN training phase, a comparison between the output forecasted by the ANN and actual data is required. To this porpoise, 15% of dataset was not used during the training phase. The 5014 data points used for validation phase have been selected randomly. Furthermore, given the complexity of the analysed phenomenon, the authors applied an optimization process: a heuristic algorithm based on natural selection and biological evolution principles that belongs to a family of optimization techniques [39]. This procedure permits to optimize the topology of the ANN and some parameters involved in the activation functions.

5.1. ANN dataset

To train the ANN, a large database of experimental data was implemented: 12 different parameters with 10-minute intervals were collected; 10 inputs and 1 output. Inputs are:

1. average hub wind speed [m/s];
2. average air density [kg/m^3];
3. relative humidity [%];
4. atmospheric pressure [Pa];
5. air temperature [°C];
6. wind direction [°];
7. turbulence percentage of wind direction [%];
8. turbulence percentage of wind speed [%];
9. wind speed gust ratio;
10. wind specific power [W/m^2].

The output data is the average output power [kW].

5.2. ANN development

After the pre-processing phase, several ANN topologies were explored. Particularly, several topologies of ANNs, varying the number of neurons belonging to the hidden layers, varying the type of activation functions, and changing the structure of the connections have been analysed. In the following Fig. 16, the configuration of the selected best ANN is sketched.

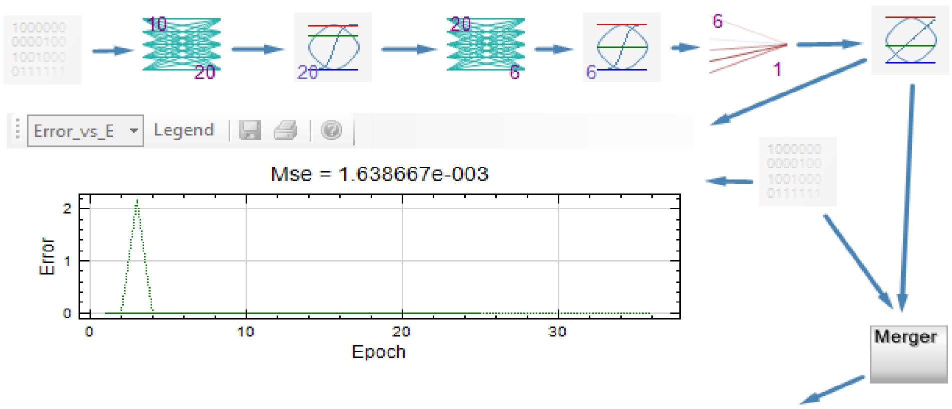

Fig. 16. Structure and topology of the selected best ANN.

This ANN is a Multilayer Perceptron (*MLP*) with Feed-forward back-propagation [40]: a network where information moves in one direction, forward, from input nodes, hidden nodes, and output nodes. More in detail, the network is organized in:

- 4 neuron layers;
- 1 input neuron layers with;
  - a neuron for each input signal (10 inputs);
- 2 neurons hidden layers; respectively of 20 and 6 neurons;
- 1 output neuron.

In Fig. 16 it also possible to observe the deviation between expected and calculated results (validation phase) that after only 40 epochs is was already close to 10^{-3}.
Among each neurons layer, it is possible to identify an activation function node that determines if the output of the layer can be propagated. In our case we used a combination of linear and hyperbolic tangent functions (tanh-sigmoid) [35]. Furthermore, different simulations have been carried out changing the epochs of the training phase.

In order to obtain a more reliable model, after the identification of the best structure, an optimization phase was conducted. The use of an evolutionary process has allowed to iteratively update the values of a set of key parameters of the network to obtain better results: learning rate (η), momentum (α) and noise level for each weight layers and type of activation functions. After the optimization phase, the best ANN topology has been trained and validated for a total of 100,000 epochs, corresponding to a computational time of about 140 hours with a machine characterized by 50 core e 200 GB of RAM.

6. RESULTS

During the post processing phase, it is possible to evaluate the goodness of the ANN model, evaluating the error between expected and calculated results. In Table 6 are collected the values of the Mean Absolute Error (MAE), Median and Standard Deviation [35]; all the quantities are expressed in kW.

Table 6: Results of the *ANN* model.

Models	Training				Validation			
	MAE	Median	StD	Confidence range 95%	MAE	Median	StD	Confidence range 95%
MLP ANN	0.697	0.793	44.015	86.278	1.119	0.985	44.529	87.294

The MAE of 0.67 kW and 1.11 kW, during the training and validation phases respectively, represent a very good result because, in both cases, practically the ANN does not overestimate or underestimate the desired result. Another important result is the StDv, indeed the range of ± 44 kW represent about 2.14 % of wind turbine nominal power.
In Fig. 17 and Fig. 18, are shown the Mean Absolute Error (MAE) frequency distribution for the training and validation phase.

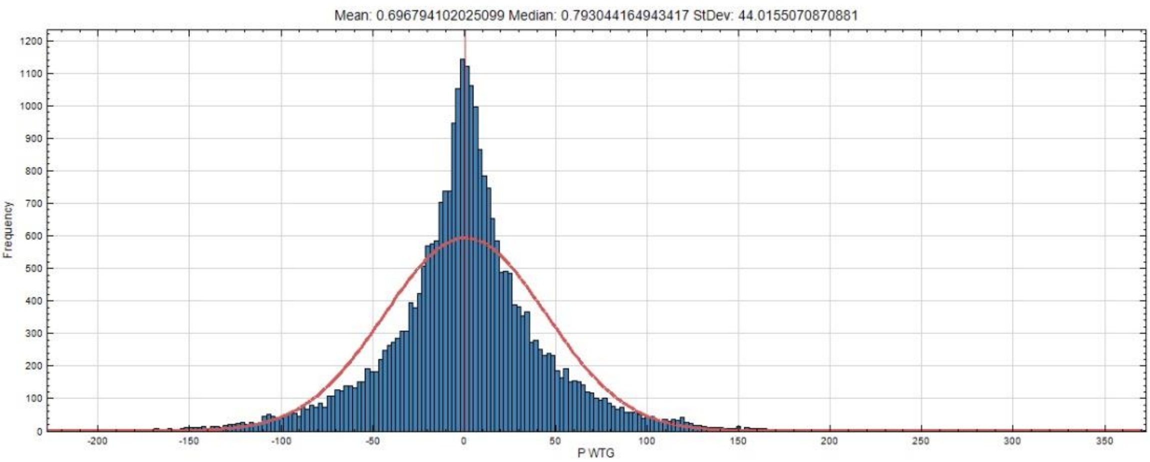

Fig. 17. MAE frequency distribution in the training phase.

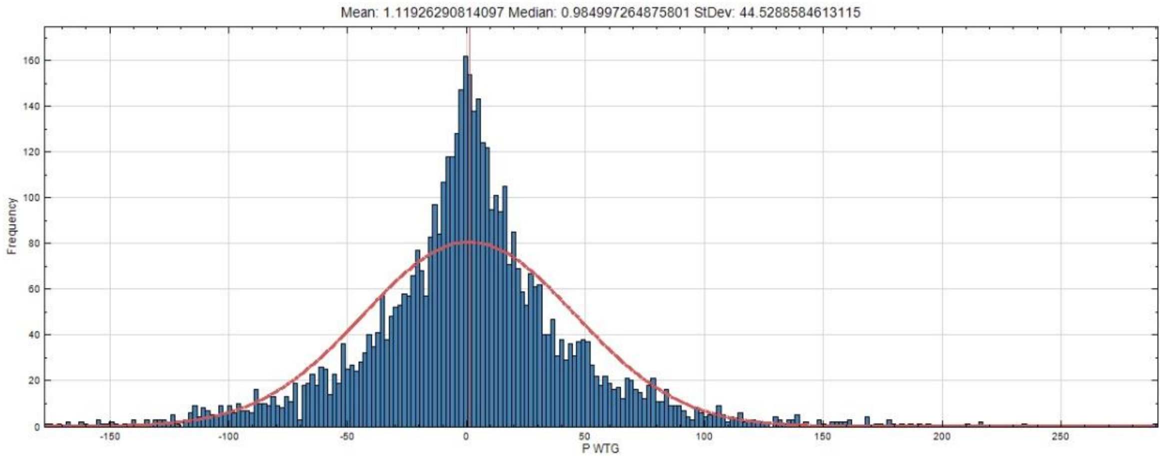

Fig. 18. MAE frequency distribution in the validation phase.

Figs. 17 and 18 show a symmetric error frequency distribution and well centred around the null value: this attests the excellent performance of the proposed neural model. The number of training epochs, although very high, did not determine the phenomenon of overfitting, for which ANNs sometimes become very good at predicting the output for the data already presented during the training phase, but they are poor in the validation phase, when are presented input values that have not been used in the training phase. Fig. 19 shows confidence plot of the power output in the range of 95% for validation dataset.

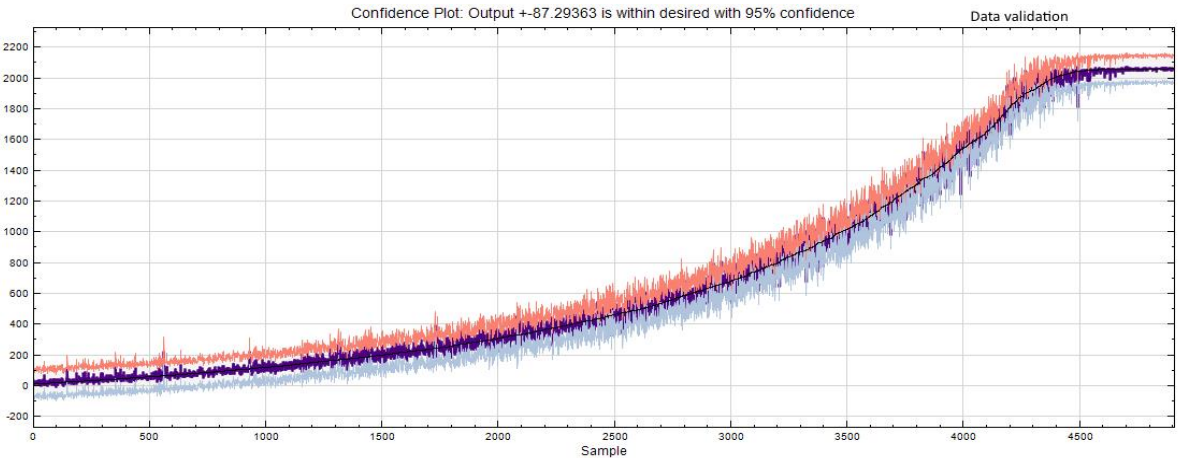

Fig.19. ANN Confidence plot for validation dataset.

The authors compared the Experimental WTPC with Fourier series interpolation (developed in the SCADA management system) with the data provided by WTPC obtained with neural network approach. In Fig. 20 is represented the comparison between the *ANN* and Fourier WTPC related the following conditions:

- average wind direction 237 [°];
- relative humidity *R.H.* = 62 %;
- air temperature *T* = 17 [°C];
- turbulence percentage of wind direction 17.5%;
- turbulence percentage of wind speed = 16.75 %;
- wind speed gust ratio = 1.43.

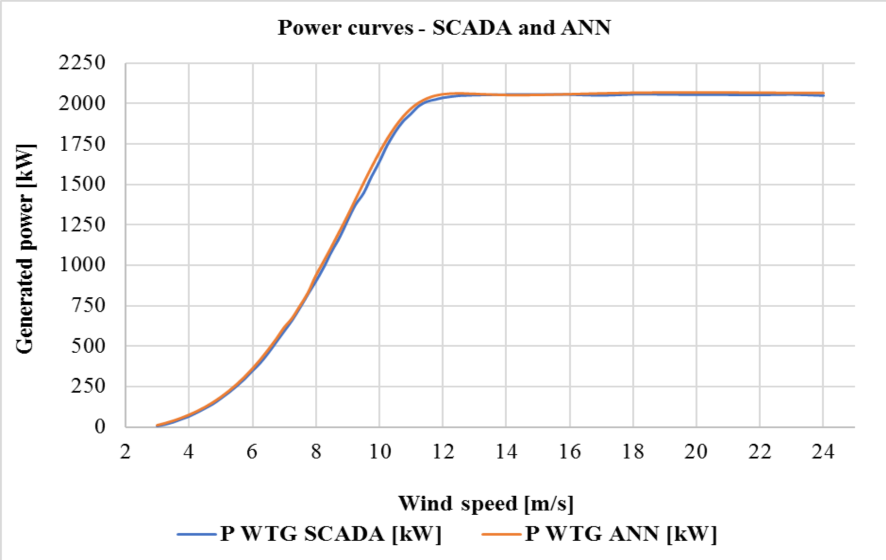

Fig. 20. ANN and SCADA WTPC.

It is important to underline how the neural model relies on a total of 10 climatic parameters, which make the model very sophisticated and accurate, with a high reliable power output calculation in any weather conditions. To generate the WTPC used for the comparison in Fig. 20, mean annual values of average wind direction, relative humidity, air temperature, turbulence percentage of wind direction, turbulence percentage of wind speed, and wind speed gust ratio have been employed.
To emphasise the high reliability of the results, in Fig. 21 and Fig. 22 are illustrated the comparison between the actual data versus the predicted data and the distribution of residuals. In Fig. 21 the prediction of the ANN fits very well with the actual power curve; all data are around the 1:1 line and the determination coefficient is close to 1.

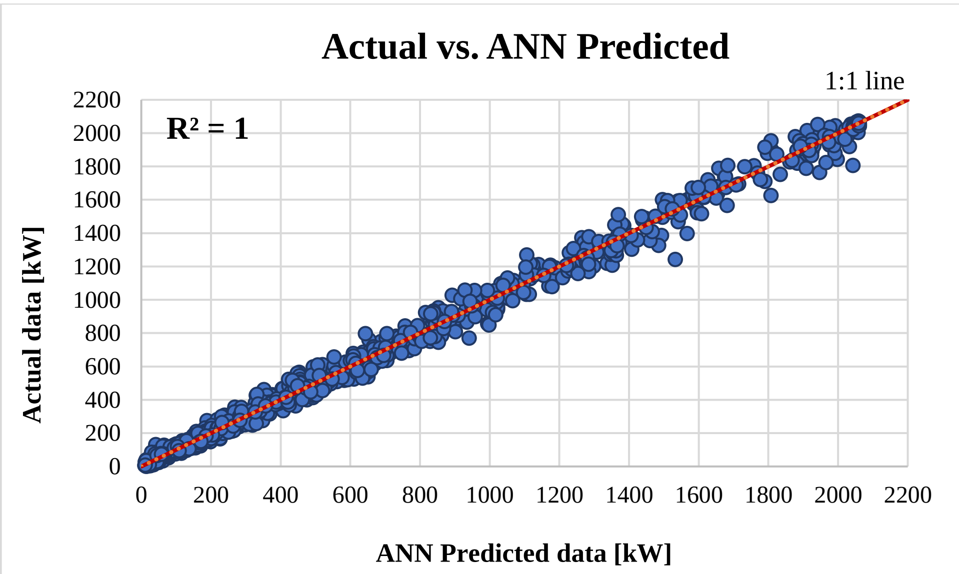

Fig. 21. Actual vs. ANN predicted data.

As displayed in the Fig. 22, the residuals do not depend on the power level considered but are of the same order of magnitude along the WTPC; in 95% of cases are within a short range of ±100 kW, about the 5% of the turbine nominal power.

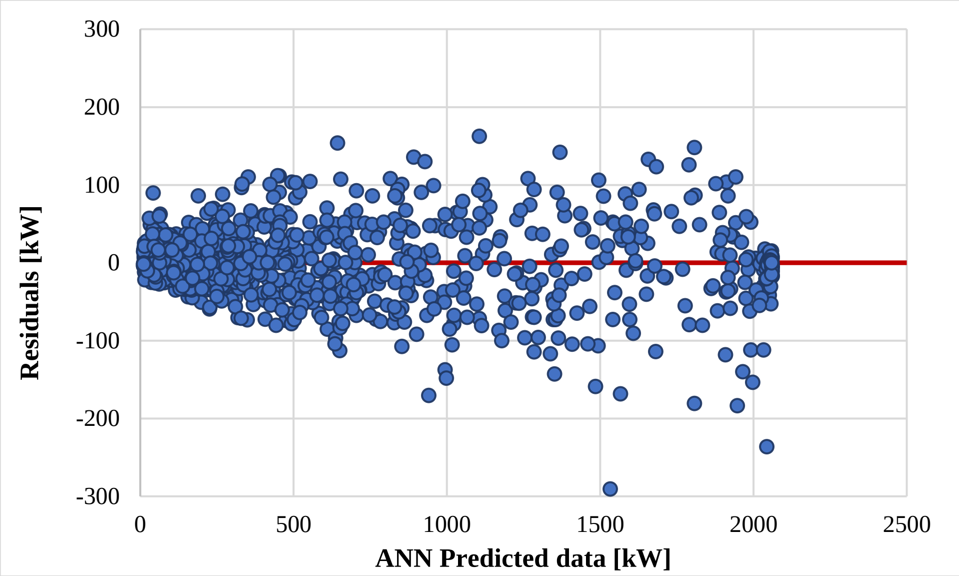

Fig. 22. Residuals distribution between the actual and predicted data.

Table 7 shows instead the comparison between the two WTPC for wind speed step of 1 m / s and the evaluation of the corresponding error in tabular form.

Table 7: Comparison between Fourier and ANN WTPC with wind speed step of 1 m/s.

Comparison between experimental WTPC for air density 1.186 kg/m³							
V_{med}	**FOURIER (8 harmonics)**	***ANN***	**Δ**	V_{med}	**FOURIER (8 harmonics)**	***ANN***	**Δ**
[m/s]	**[kW]**	**[kW]**	**[%]**	**[m/s]**	**[kW]**	**[kW]**	**[%]**
3.00	13.97	8.28	-40.73%	14.00	2057.29	2054.87	-0.12%
4.00	70.32	72.56	3.19%	15.00	2057.21	2055.22	-0.10%
5.00	177.03	182.32	2.99%	16.00	2057.46	2059.79	0.11%
6.00	344.67	358.91	4.13%	17.00	2055.56	2064.78	0.45%
7.00	586.90	613.89	4.60%	18.00	2058.00	2068.42	0.51%
8.00	894.30	936.10	4.67%	19.00	2057.55	2070.32	0.62%
9.00	1267.59	1306.94	3.10%	20.00	2057.29	2070.69	0.65%
10.00	1634.88	1698.34	3.88%	21.00	2056.20	2070.04	0.67%
11.00	1929.67	1971.29	2.16%	22.00	2055.32	2068.67	0.65%
12.00	2034.96	2059.42	1.20%	23.00	2056.21	2067.69	0.56%
13.00	2052.98	2061.78	0.43%	24.00	2051.67	2066.93	0.74%

Δ Average value for different wind velocity range		
wind speed range	**3 - 24 [m/s]**	-0.26%
wind speed range	**10 - 24 [m/s]**	0.83%
wind speed range	**13 - 24 [m/s]**	0.43%

In this case the percentage deviations are slightly greater than those evaluated from the comparison between the WTPC obtained by the cubic spline and Fourier series interpolation.

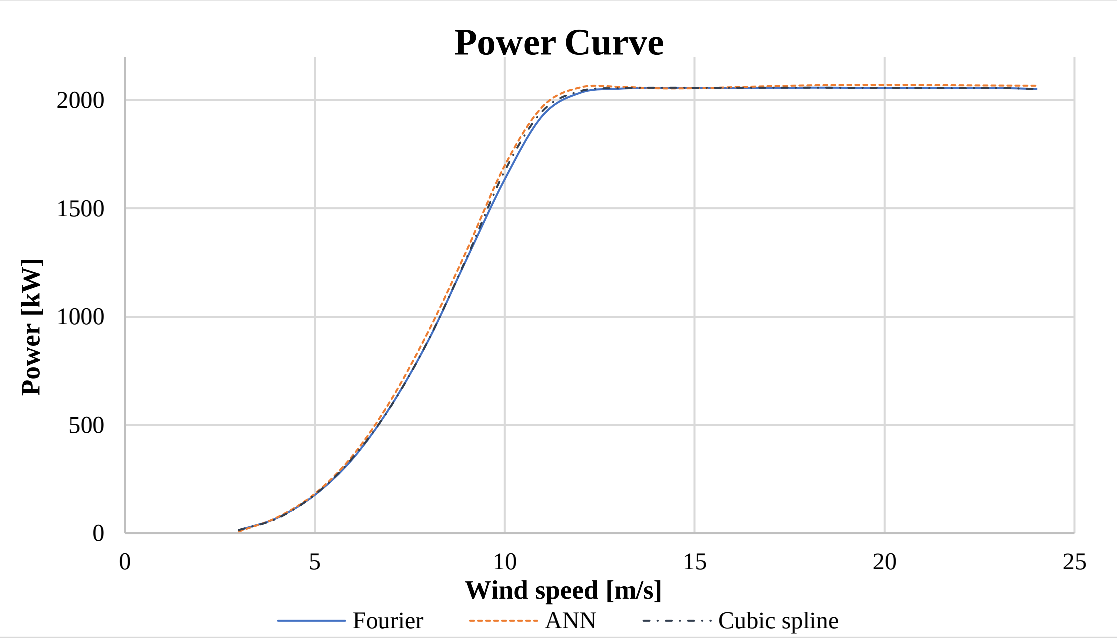

Fig.23. Comparison among the Fourier (manufacturer), ANN and cubic spline (Model 2) derived WTPC.

As example, in Fig. 23 is illustrated the comparison among: the Fourier application of issued WTPC, the ANN WTPC and the spline WTPC of the Model 2. The simultaneously comparison among the three models, with fixed air density value, and the results predicted in the same conditions by the ANN, gives rise to graphs with practically overlapping curves, which are not useful for understanding. Furthermore, it is important to underline the manner in which the neural algorithm is much more accurate and flexible because allows to consider variable climate and different physical weather conditions at the same time, instead the curves of the three models would allow to plotting only constant density trends.

7. Conclusion

The field of research concerning the truthfulness and reliability of Wind Turbine Power Curves is very important for designers but especially for investors. Small discrepancies between the declared technical characteristics and the actual characteristics of the turbine can lead to substantial errors in the assessment of energy productivity. For this reason, it is important to have reliable mathematical procedures that allow to deduce the WTPC from the experimental data so that the investors and the plant management can compare the actual characteristics with those declared by the producers.

Based on this observation, two different approaches were studied to define WTPCs using one year of monitored data over a commercial real plant. In particular, in this work have been presented a simplified mathematical approach based on the elaboration of wind speed data and power output with two different interpolation procedures, and a neural approach that allows to immediately calculate the actual power curve taking into account simultaneously many more climatic variables that influences the electric power generation.

The simplified mathematical approach involved the generation of three distinct models which were developed on the basis of data recorded by a wind turbine SCADA monitoring system.

These models therefore allow to determine the WTPC according to the wind speed and to the value of the air density. The first model takes into account a variability range of air density, the second considers a fixed air density value, and the third model issues the WTPC taking into account two constant seasonal values of air density. The generated power curves, have been compared with those one officially issued by the manufacturer.
To make possible this comparison, being the WTPCs supplied by the manufacturer characterized by a wind speed step of 1 m/s, it was necessary to interpolate the values obtaining a new wind speed step of 0.1 m/s. The reliability of WTPC based on Fourier series interpolation it was assessed even by comparing the energy expected and produced by the plant.
The neural network approach, thanks to its ability to solve complex problems, has allowed the development of a mathematic tool able to quickly and reliably predict the WTPC employing the dataset of climatic variables that are normally always recorded by the SCADA system of the wind turbine.
A further comparison was made between the WTPC obtained from the ANN and those one obtained with Fourier series interpolation. The results of both methods show that the developed instrument can predict turbine power with a minimum error. The strength of the ANN tool instrument relies in the high reliability of the forecasted power output even with limited input dataset. In particular, unlike other simplified models, which are often already available in the management software of wind power plants, the proposed approach is able to employ many more interesting parameters in a simple and immediate way, obtaining a very good evaluation of the producibility.
The possibility to use an extremely reliable instrument in assessing the WTPC in many different weather conditions allows to help the operators of wind farms in demonstrating a possible deviation of the wind turbine energy performances with respect to the official data declared by the manufacturer. The ascertainment of this deviation can in fact mean, for the producer the payment of huge penalties, and for the owner the recovery of lost revenues due to an erroneous evaluation of the energy producibility.

References

[1] B. Manobel, F. Sehnke, J.A. Lazzús, I. Salfate, M. Felder, S. Montecinos, Wind turbine power curve modeling based on Gaussian Processes and Artificial Neural Networks, Renew. Energy. 125 (2018) 1015–1020. doi:10.1016/j.renene.2018.02.081.

[2] I. Pineda, W. Pierre Tardieu, 2016 European statistics WindEurope Business Intelligence Aloys Nghiem (Installation highlights) Ariola Mbistrova (Financing highlights) ediTors: Courtesy of Senvion Gmbh WindeuroPe acknoWledges The kind cooPeraTion of The folloWing associaTions and insTi, 2017. https://windeurope.org/wp-content/uploads/files/about-wind/statistics/WindEurope-Annual-Statistics-2016.pdf (accessed November 13, 2018).

[3] R. Belu, D. Koracin, Wind characteristics and wind energy potential in western Nevada, Renew. Energy. 34 (2009) 2246–2251. doi:10.1016/j.renene.2009.02.024.

[4] K. Xie, R. Billinton, Energy and reliability benefits of wind energy conversion systems, Renew. Energy. 36 (2011) 1983–1988. doi:10.1016/j.renene.2010.12.011.

[5] J.F. Manwell, J.G. McGowan, A.L. Rogers, Wind Energy Explained: Theory, Design and Application, 2010. doi:10.1002/9781119994367.

[6] R. Veena, V. Femin, S. Mathew, I. Petra, J. Hazra, Intelligent models for the power curves of small wind turbines, in: Proc. 2016 Int. Conf. Cogener. Small Power Plants Dist. Energy, ICUE 2016, 2016. doi:10.1109/COGEN.2016.7728965.

[7] T. Burton, Wind energy handbook, Wiley, 2011. https://books.google.it/books?hl=it&lr=&id=dip2LwCRCscC&oi=fnd&pg=PT8&dq=Wind+Energy+Handbook,+Wiley,+2001&ots=IdBFTxJrFd&sig=0BnOv1ekClxDuStoi

bvrw4PODaM#v=onepage&q=Wind Energy Handbook%2C Wiley%2C 2001&f=false (accessed November 13, 2018).

[8] S. Frandsen, I. Antoniou, J.C. Hansen, L. Kristensen, H.A. Madsen, B. Chaviaropoulos, D. Douvikas, J.A. Dahlberg, A. Derrick, P. Dunbabin, R. Hunter, R. Ruffle, D. Kanellopoulos, G. Kapsalis, Redefinition power curve for more accurate performance assessment of wind farms, Wind Energy. 3 (2000) 81–111. doi:10.1002/1099-1824(200004/06)3:2<81::AID-WE31>3.0.CO;2-4.

[9] C. Carrillo, A.F. Obando Montaño, J. Cidrás, E. Díaz-Dorado, Review of power curve modelling for windturbines, Renew. Sustain. Energy Rev. (2013). doi:10.1016/j.rser.2013.01.012.

[10] M. Lydia, S.S. Kumar, A.I. Selvakumar, G.E. Prem Kumar, A comprehensive review on wind turbine power curve modeling techniques, Renew. Sustain. Energy Rev. 30 (2014) 452–460. doi:10.1016/j.rser.2013.10.030.

[11] M. Lydia, A.I. Selvakumar, S.S. Kumar, G.E.P. Kumar, Advanced algorithms for wind turbine power curve modeling, IEEE Trans. Sustain. Energy. 4 (2013) 827–835. doi:10.1109/TSTE.2013.2247641.

[12] J. Gottschall, J. Peinke, How to improve the estimation of power curves for wind turbines, Environ. Res. Lett. 3 (2008). doi:10.1088/1748-9326/3/1/015005.

[13] F. Pelletier, C. Masson, A. Tahan, Wind turbine power curve modelling using artificial neural network, Renew. Energy. 89 (2016) 207–214. doi:10.1016/j.renene.2015.11.065.

[14] International Electrotechnical Commission, Wind turbines, Part 12-1: Power performance measurements of electricity producing wind turbines, Int. Electrotech. Comm. (2005). doi:10.1109/ICIP.2001.958192.

[15] International Electrotechnical Commission, Wind Turbines – Part 12-2: Power Performance of Electricity-producing Wind Turbines Based on Nacelle Anemometry, Int. Electrotech. Comm. (2013).

[16] A. Albers, T. Jakobi, R. Rohden, J. Stoltenjohannes, Influence of meteorological variables on measured wind turbine power curves, in: Eur. Wind Energy Conf. Exhib. 2007, EWEC 2007, 2007: pp. 1730–1736.

[17] E. Sainz, A. Llombart, J.J. Guerrero, Robust filtering for the characterization of wind turbines: Improving its operation and maintenance, Energy Convers. Manag. 50 (2009) 2136–2147. doi:10.1016/j.enconman.2009.04.036.

[18] E. Gonzalez, B. Stephen, D. Infield, J.J. Melero, Using high-frequency SCADA data for wind turbine performance monitoring: A sensitivity study, Renew. Energy. 131 (2019) 841–853. doi:10.1016/j.renene.2018.07.068.

[19] J. Nilsson, L. Bertling, Maintenance management of wind power systems using condition monitoring systems - Life cycle cost analysis for two case studies, IEEE Trans. Energy Convers. (2007). doi:10.1109/TEC.2006.889623.

[20] D. McMillan, G.W. Ault, Quantification of condition monitoring benefit for offshore wind turbines, Wind Eng. 31 (2007) 267–285. doi:10.1260/030952407783123060.

[21] A. May, D. McMillan, S. Thöns, Economic analysis of condition monitoring systems for offshore wind turbine sub-systems, IET Renew. Power Gener. 9 (2015) 900–907. doi:10.1049/iet-rpg.2015.0019.

[22] F.P. García Márquez, A.M. Tobias, J.M. Pinar Pérez, M. Papaelias, Condition monitoring of wind turbines: Techniques and methods, Renew. Energy. 46 (2012) 169–178. doi:10.1016/j.renene.2012.03.003.

[23] W. Yang, P.J. Tavner, C.J. Crabtree, Y. Feng, Y. Qiu, Wind turbine condition monitoring: Technical and commercial challenges, Wind Energy. 17 (2014) 673–693. doi:10.1002/we.1508.

[24] J. Tautz-Weinert, S.J. Watson, Using SCADA data for wind turbine condition

monitoring - A review, IET Renew. Power Gener. 11 (2017) 382–394. doi:10.1049/iet-rpg.2016.0248.

[25] S. Li, D.C. Wunsch, E. O'Hair, M.G. Giesselmann, Comparative analysis of regression and artificial neural network models for wind turbine power curve estimation, J. Sol. Energy Eng. Trans. ASME. 123 (2001) 327–332. doi:10.1115/1.1413216.

[26] G. Grassi, P. Vecchio, Wind energy prediction using a two-hidden layer neural network, Commun. Nonlinear Sci. Numer. Simul. 15 (2010) 2262–2266. doi:10.1016/j.cnsns.2009.10.005.

[27] M. Carolin Mabel, E. Fernandez, Analysis of wind power generation and prediction using ANN: A case study, Renew. Energy. 33 (2008) 986–992. doi:10.1016/j.renene.2007.06.013.

[28] F. Sehnke, A. Strunk, M. Felder, J. Brombach, A. Kaifel, J. Meis, Wind power resource estimation with deep neural networks, 2013. doi:10.1007/978-3-642-40728-4_70.

[29] A. Kusiak, H. Zheng, Z. Song, Models for monitoring wind farm power, Renew. Energy. 34 (2009) 583–590. doi:10.1016/j.renene.2008.05.032.

[30] Li, Shuhui, Artificial neural networks applied for wind power estimation and forecast, Texas Tech University, 1999. https://dl.acm.org/citation.cfm?id=930249 (accessed November 7, 2018).

[31] Z.-Q. Wu, W.-J. Jia, L.-R. Zhao, C.-H. Wu, Maximum wind power tracking based on cloud RBF neural network, Renew. Energy. 86 (2016) 466–472. doi:10.1016/j.renene.2015.08.039.

[32] X. Qing, Statistical analysis of wind energy characteristics in Santiago island, Cape Verde, Renew. Energy. 115 (2018) 448–461. doi:10.1016/j.renene.2017.08.077.

[33] S.K. Najid, A. Zaharim, A.M. Razali, M.S. Zainol, K. Ibrahim, K. Sopian, Analyzing the east coast Malaysia wind speed data, Int. J. Energy Environ. 3 (2009) 53–60.

[34] V. Lo Brano, A. Orioli, G. Ciulla, S. Culotta, Quality of wind speed fitting distributions for the urban area of Palermo, Italy, Renew. Energy. 36 (2011) 1026–1039. doi:10.1016/j.renene.2010.09.009.

[35] G. Ciulla; A. D'Amico;V. Lo Brano; M. Beccali, ANN Decision Support Tool for the prediction of the Thermal Energy Performance of European Top Rated Energy Efficient Non-residential Buildings, in: Sustain. Dev. Energy, Water Environ. Syst., Dubrovnik, 2017.

[36] V. Lo Brano, G. Ciulla, M. Di Falco, Lo Brano V, Ciulla G, Di Falco M, V. Lo Brano, G. Ciulla, M. Di Falco, Artificial neural networks to predict the power output of a PV panel, Int. J. Photoenergy. 2014 (2014) 1–12. doi:10.1155/2014/193083.

[37] V. Pacelli, M. Azzollini, An artificial neural network approach for credit risk management, J. Intell. Learn. Syst. Appl. 3 (2011) 103.

[38] S. Haykin, Neural Networks: A Comprehensive Foundation, 1st ed., Prentice Hall PTR, Upper Saddle River, NJ, USA, 1994.

[39] D. Floreano, C. Mattiussi, Manuale sulle reti neurali, 2002.

[40] A. El Shahat, R.J. Haddad, Y. Kalaani, An artificial Neural Network model for wind energy estimation, in: Conf. Proc. - IEEE SOUTHEASTCON, 2015. doi:10.1109/SECON.2015.7133044.